Development of simple algorithms for the detection of fecal contaminants on apples from visible/near infrared hyperspectral reflectance imaging

ARTICLE *in* JOURNAL OF FOOD ENGINEERING · FEBRUARY 2007

Impact Factor: 2.77 · DOI: 10.1016/j.jfoodeng.2006.11.018

5 AUTHORS, INCLUDING:

Yongliang Liu
Agricultural Research Service
82 PUBLICATIONS **1,493** CITATIONS

SEE PROFILE

Available online at www.sciencedirect.com
ScienceDirect
Journal of Food Engineering 81 (2007) 412–418
JOURNAL OF FOOD ENGINEERING
www.elsevier.com/locate/jfoodeng

Development of simple algorithms for the detection of fecal contaminants on apples from visible/near infrared hyperspectral reflectance imaging ☆

Yongliang Liu [a], Yud-Ren Chen [b,*], Moon S. Kim [b], Diane E. Chan [b], Alan M. Lefcourt [b]

[a] Department of Biosystems and Agricultural Engineering, University of Kentucky, Lexington, KY 40546, United States
[b] Instrumentation and Sensing Laboratory, Henry A. Wallace Beltsville Agricultural Research Center, USDA, Building 303, BARC-East, 10300 Baltimore Avenue, Beltsville, MD 20705, United States

Received 29 June 2006; received in revised form 8 November 2006; accepted 16 November 2006
Available online 2 January 2007

Abstract

Hyperspectral reflectance images of two cultivars of apples were acquired after fecal treatments at three different concentrations to explore the potential for the detection of fecal contaminants on apple surfaces. Region of interest (ROI) spectral features of fecal contaminated areas showed a reduction in reflectance intensity compared to those of uncontaminated skins. Large spectral differences between uncontaminated and fecal contaminated skins of two types of apples occurred in the 675–950 nm visible/NIR region, which provided the basis for developing universal algorithms in the detection of fecal spots. Comparison of a number of processed images revealed that a dual-band ratio ($Q_{725/811}$) algorithm could be used to identify fecal contaminated skins effectively. The result was most important as the two bands are away from the absorptions of natural pigments (such as chlorophylls and carotenoids), and hence can reduce the influence from color variations due to different apple cultivars.

Keywords: Hyperspectral imaging spectroscopy; Image processing; Algorithm; Principal component analysis; Apple; Fecal contamination; Food safety

1. Introduction

Contamination of apple products with bacterial food-borne pathogens can potentially occur as a result of exposure of apples to fecal materials during the growing and harvesting phases. Animal feces are the most likely source of pathogenic *E. coli* O157: H7 contamination. In addition, the potential of contamination increases with physical damages on apples, such as lesions and bruises, which provide a site for bacterial growth. Cleaning processes can reduce, but are unlikely to eliminate, pathogens from the surfaces of produce even if antimicrobial chemicals are contained in the wash water (FDA, 1998). Bacterial pathogens can be transmitted to humans by consumption of contaminated apples or raw (unpasteurized) apple juice/cider. There have been several reported food-borne illness outbreaks attributed to unpasteurized apple juice and cider (CDC, 1996, 1997). These outbreaks have raised the concerns of public health officials and apple cider/juice producers.

To ensure healthy and safe apple products to the consumers, the US Food and Drug Administration (FDA) has issued an HACCP system to minimize the likelihood of bacterial pathogens in fruit juices, and also identified an urgent need to develop methods for the detection of fecal matters on apples (FDA, 2001). Preventing apples with visible fecal contamination from entering the washer tank is critical for preventing cross-contamination of other apples. Thus, removal of fecal contaminated apples, before

☆ Mention of a product or specific equipment does not constitute a guarantee or warranty by the US Department of Agriculture and does not imply its approval to the exclusion of other products that may also be suitable.

* Corresponding author. Tel.: +1 301 504 8450; fax: +1 301 504 9466.
E-mail address: Cheny@ba.ars.usda.gov (Y.-R. Chen).

0260-8774/$ - see front matter © 2006 Elsevier Ltd. All rights reserved.
doi:10.1016/j.jfoodeng.2006.11.018

entering the washing pool, has been suggested by FDA guidance on good agricultural practices (GAPs) and good manufacturing practices (GMPs) for fruits and vegetables (FDA, 1998).

Currently, inspection of fecal contamination is through visual observation over an inspection table. Inspectors use the guidelines of Current Good Manufacturing Practices (CGMPs) to prevent apples with visible fecal contaminants from entering the next step. Current visual inspection is labor intensive and prone to human error and inspector-to-inspector variation. Therefore, researchers at the US Department of Agriculture (USDA) Agricultural Research Services have been developing hyperspectral reflectance imaging system for the detection of fecal contaminated apples (Kim et al., 2002; Mehl, Chao, Kim, & Chen, 2002; Mehl, Chen, Kim, & Chan, 2004). The preliminary results have demonstrated that spectral imaging technique can be used effectively for detecting fecal spots on apples in the visible and near-infrared (NIR) region.

To implement hyperspectral reflectance imaging in potential on-line inspection, less spectral bands (usually two or three) were selected for the design of rapid sensing instruments; namely multispectral imaging systems. From hyperspectral reflectance imaging spectra, the essential bands were obtained through a number of data analysis, such as performing principal component analysis (Kim, Chen, & Mehl, 2001), and observing the separations visually on images at specific wavelengths (Mehl et al., 2004). The representative bands should not only reflect the chemical/physical information, but also maintain the successive discrimination and classification efficiency.

The main objectives of this study were to obtain the characteristic bands for fecal contaminated apples and to develop simple algorithms for the detection of fecal spots. The ultimate purpose was to lead to the development of faster and more efficient multispectral techniques for real-time inspection of fecal contaminants for apple related product safety.

2. Materials and methods

2.1. Apples and fecal contamination treatments

A number of two cultivars of apples (Golden Delicious and Red Delicious) were collected from containers that were used to store the harvested apples in Pennsylvania (Rice Fruit Co., Gardners, PA). The apples were transported to the Laboratory in Beltsville, MD, and kept in a cold storage room (2–4 °C). To address the variations among the apples, 96 apples from each cultivar were used randomly.

Cattle feces were selected to represent the fecal contaminant, as it is one of the most common sources of fecal contamination (Cody et al., 1999). Fresh cow feces were obtained from a pasture at USDA Beltsville dairy facility in Maryland. They were diluted with drinkable water (H_2O) to produce three different concentrations of 50%, 5%, and 0.5% (weight/weight, w/w). Then, three fecal spots were formed by applying three solutions to one side of each apple with the use of a pipette. After the evaporation of water, two fecal spots in circles, with the size of around 1 cm in diameter, were observed clearly. The apparent two spots represented the deposition from two concentrated solutions, 50% and 5%, respectively. For the collection of images, a set of 12 fecal treated apples was placed on a tray painted with non-fluorescent, flat black paint to minimize background scattering.

2.2. Hyperspectral imaging acquisition and image analysis

A hyperspectral reflectance imaging system developed by the USDA Instrumentation and Sensing Laboratory was used to scan the apples (Kim et al., 2001). It was operated in a line-by-line scan spectrograph with a spectral resolution of approximately 7-nm full width at half maximum (FWHM). A thermo-electrically cooled electron multiplying charge-coupled device (EMCCD) camera with 288 (vertical) × 560 (horizon) pixels (Andor, Inc., South Windsor, Conn.) was used, and the effective spectral and spatial dimensions were limited to 112 pixels (channels) with 2× binning and 460 pixels without binning, respectively. It produced an image cube of 460 × 1200 spatial and 112 spectral bands for each group of 12 apples. The spectral wavelength range was in visible/NIR region of 447–951 nm with a 4.5 nm interval. Two 150 W halogen lamps were applied to provide the illumination for image collection. A Spectralon™ white reference panel with nearly 99% reflectance (Labsphere, North Sutton, NH, USA) was employed as a reference. The camera dark image and the white reflectance image were recorded prior to the acquisition of the hyperspectral images. During the scanning process, room lights were turned off to prevent interference from ambient light.

In-house laboratory-developed software (Kim et al., 2001) and the commercial ENVI 3.2 software package (Research Systems, Inc., Boulder, CO) were used for the analysis of hyperspectral images. Prior to algorithm and principal component image analysis, images at 665 nm were processed with binary function at a threshold of 0.4% of reflectance intensity to create a mask for the apple surface in each image. The threshold value was determined by visual observation so as to exclude the image background.

During principal component analysis (PCA) of images, a correlation matrix of the image is calculated (Lay, 2002). Then this correlation matrix, a diagonal matrix, is used to compute the eigenvalues. The eigenvalues are equivalent to the variance of each principal component (PC) image. These PC images are ordered in the decreasing degree of variance sizes, where first PC accounts for the largest variance. Hence, PCA transforms the original data set into a set of new un-correlated linear combinations of the original data with much less variables.

3. Results and discussion

3.1. Hyperspectral reflectance images of fecal contaminated apples

Fig. 1 shows the representative reflectance images, at 675 nm and 811 nm, of Golden Delicious apples contaminated with three fecal solutions. Images at these wavelengths were selected for comparison, because the 675 nm band originates from the chlorophyll component in both apple and feces, while the 811 nm band shows great intensity variations (as indicated in Figs. 2 and 3) and is not associated with colorant. At least one fecal contaminant (in black circles) was clearly identified on each apple, with black circled spots corresponding to the larger amount of feces (50% w/w) on apple surfaces and white circled spots to the lower amount of feces (5% w/w) on apples. Noticeably, few spots (in broken black circles) resulting from the depositions of 0.5% w/w fecal solution were indicated, probably due to the sensitivity and detection limit of camera in this spectral range. In other words, appearance of fecal spots in images was consistent with that from visual observation. In separate studies, Kim et al. reported the potential of hyperspectral fluorescence imaging in the detection of fecal matters on apples and cantaloupes, with the amount of as low as 16-μg/ml dry fecal matter and the minimum concentration of 0.5% (or 1:200) feces solution by forming fecal spots of 1 cm in diameter (Kim et al., 2002; Vargas et al., 2005).

Fig. 1 suggested that both uncontaminated and fecal contaminated apple skins were showing lighter intensities at 811 nm image than at 675 nm image, and thin fecal spots (non-black circles) were relatively difficult to be defined from the 811 nm image. However, by examining the images of a variety of Golden Delicious apples, it was observed that the 811 nm images might provide slightly better separation result between uncontaminated and fecal contaminated skins than the 675 nm images. The reason was that the use of 811 nm band, which is in NIR region and includes comprehensive contributions from the third overtones of C–H/N–H/O–H stretching modes of organic constitutes in feces and apple skins (Osborne, Fearn, & Hindle, 1993), can avoid the effect of natural pigments (chlorophylls and carotenoids) on the discrimination analysis, by reducing the variations of color from one apple to another.

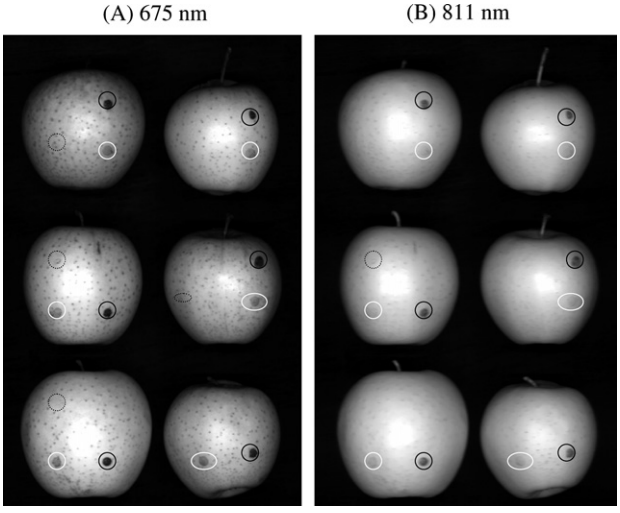

Fig. 1. Hyperspectral images, at (A) 675 nm and (B) 811 nm, of Golden Delicious apples contaminated with three feces solutions of 50% (in black circles), 5% (in white circles), and 0.5% (in broken black circles).

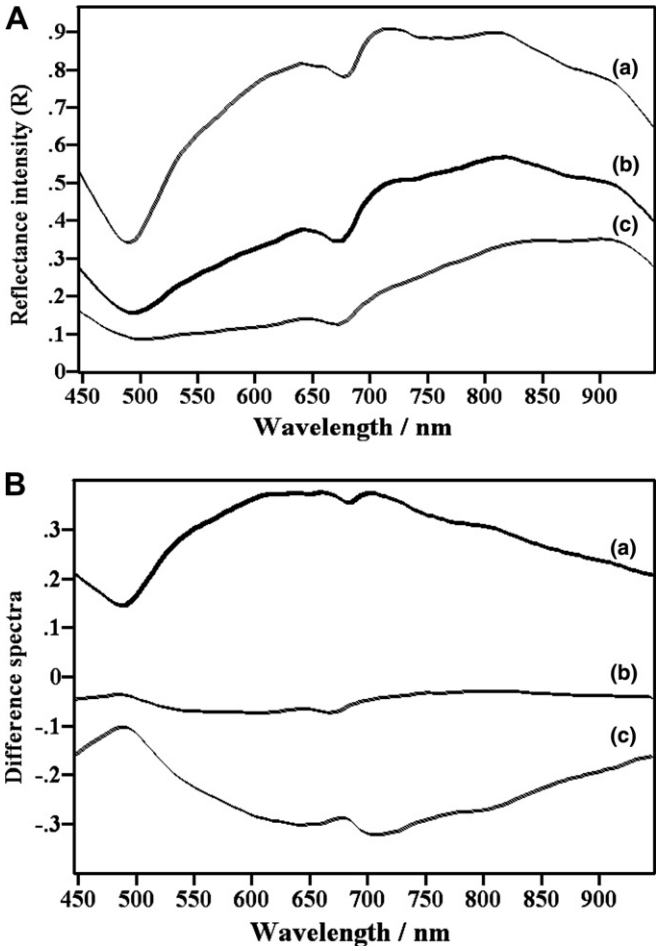

Fig. 2. (A) Representative ROI reflectance spectra of uncontaminated Golden Delicious apple skins (a), thin (b), and thick (c) fecal contaminated apple skins; (B) ROI difference spectra of uncontaminated (a), thin (b), and thick (c) fecal contaminated apple skins.

3.2. Spectral characteristics of uncontaminated and fecal contaminated apple skins

Fig. 2A shows average regions of interest (ROIs) reflectance spectra of uncontaminated apple skins (a), thin (b) and thick (c) fecal contaminated skins in the 450–950 nm region, extracted from the images of a number of Golden Delicious apples. From individual images, ROIs were chosen from 3 different locations on apple surfaces: (1) uncontaminated skins at the center of each apple, (2) thin fecal contaminated skins (non-black spots), and (3) thick fecal contaminated skins (black spots). ROI areas, varying in

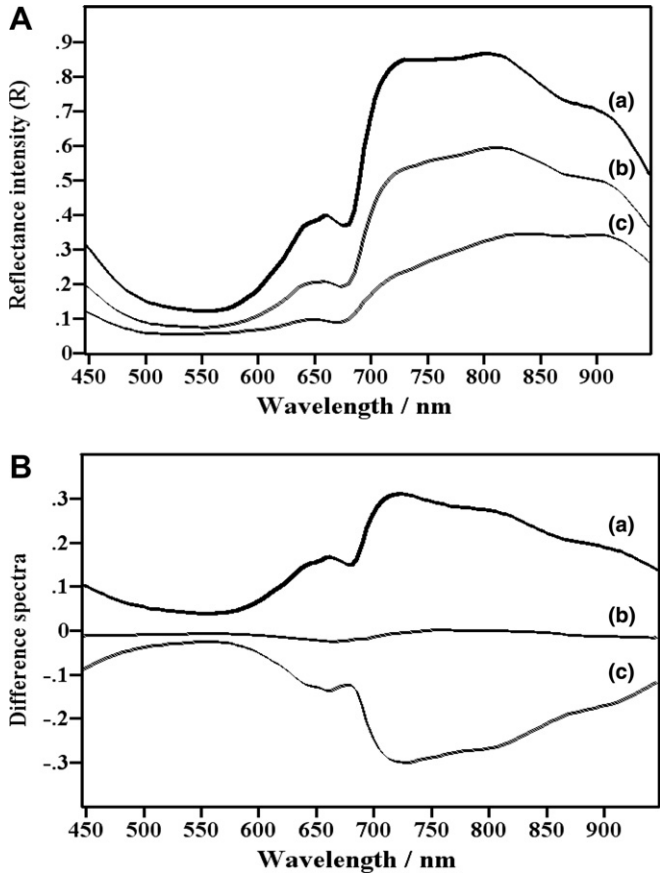

Fig. 3. (A) Representative ROI reflectance spectra of uncontaminated Red Delicious apple skins (a), thin (b), and thick (c) fecal contaminated apple skins; (B) ROI difference spectra of uncontaminated (a), thin (b), and thick (c) fecal contaminated apple skins.

size from 16 to 100 pixels and being smaller than actual fecal spots, were selected by using the rectangle and drawing point modes of ENVI software.

The relative reflectance intensity was clearly observed to decrease over the entire spectral region from uncontaminated skins to thin and thick fecal contaminated ones. Major difference was shown in the 475–850 nm range, and apparently it was feces that caused such intensity reduction. On the other hand, a common and sharp absorption band near 675 nm indicated the existence of chlorophyll *a* species in both uncontaminated and fecal contaminated skins. It was reasonable to observe a relatively weak 675 nm band in thick fecal spot (Fig. 2A (c)), due to the fact that chlorophyll pigment in feces was likely from undigested feedstuff. Meanwhile, reflectance curve of thin fecal spot given in Fig. 2A (b) was between those of uncontaminated skin and thick fecal spot. If the amounts or concentrations of fecal contaminants were very low, spectral features of fecal spots would be very similar to those of uncontaminated skins, making the detection of trace feces very difficult.

Fig. 2B shows difference spectra that were calculated by subtracting the average spectrum of the three ROI spectra in Fig. 2A from each spectrum. The difference spectra clearly indicated the large variations in the 525–850 nm region between uncontaminated and fecal contaminated skins. There are at least 4 peaks near 490, 642, 715, and 811 nm which had maximum/minimum difference intensities. In general, relative reflectance intensity at 490 nm increased while those at 642, 715, and 811 nm decreased from uncontaminated apple skins to fecal contaminated ones.

To address differences in coloration due to different cultivars, Red Delicious apples were selected for comparison. Fig. 3A shows the ROI reflectance spectra of uncontaminated, thin and thick fecal contaminated skins from the images of a number of Red Delicious apples. Similar to the pattern in Fig. 2A, relative reflectance intensities were found to decrease from uncontaminated Red Delicious apple skins to thin and thick fecal contaminated ones.

Common features between uncontaminated Golden Delicious and Red Delicious apples (Figs. 2A and 3A) included the spectral intensity reduction from uncontaminated to fecal contaminated skins and a distinctive absorption band around 675 nm. Meanwhile, thin fecal spot on Golden Delicious apples showed nearly identical curve as that on Red Delicious apples, so did thick fecal spot. Expectedly, obvious spectral differences between two types of apples occurred in the 525–625 nm region, due to the color appearance of different cultivars.

Difference spectra in Fig. 3B suggested the large variations in the 675–850 nm region between uncontaminated and fecal contaminated Red Delicious apple skins. There existed at least 3 peaks near 557, 725, and 811 nm at which great intensity variations occurred. Comparison of difference spectra between Figs. 2B and 3B revealed the similarity in 675–950 nm region, which might be important in the development of universal and simple algorithms for different apple cultivars. Also, it indicated the discrepancy in 450–675 nm, which was caused by the changes of relative amount of pigments (e.g. chlorophylls and carotenoids) in Golden and Red Delicious apples.

3.3. Comparison of dual-band algorithms, second difference, and PCA models for the detection of fecal contaminants on Golden Delicious apples

The above ROI spectral analysis revealed at least six characteristic bands at 490, 557, 642, 715, 725, and 811 nm for two types of apples, and these bands could be used for the detection of fecal contaminated spots. To develop robust and rapid multispectral imaging systems suitable for any apple cultivars, less spectral bands were desired. Therefore, we developed a number of algorithms, on the basis of three bands at 557, 725, and 811 nm, to analyze the images of Golden and Red Delicious apples.

Two-band ratio ($Q_{725/557}$) given in Eq. (1) was associated with the color appearance of apples and might provide the separation effect:

$$Q_{725/557} = R_{725}/R_{557} \quad (1)$$

where $Q_{725/557}$ represents a quotient of spectral reflectances, and R_{725} nm and R_{557} nm are reflectance intensities at 725 nm and 557 nm, respectively.

The dual-band ratio ($Q_{725/557}$) algorithm images are given in Fig. 4A. Although the $Q_{725/557}$ algorithm images showed clear fecal spots (in white circled), they did not suggest much promise in the detection of fecal spots, because some uncontaminated portions were misclassified as fecal contaminated ones.

Alternatively, the 557 nm visible band was replaced by a 811 nm NIR band, and the processed images were shown in Fig. 4B with the use of new ratio $Q_{725/811}$ algorithm. It can be seen that two kinds of fecal spots (shown in dark) were apparently discriminated from uncontaminated skins (shown in white), with thick feces in black circles and thin feces in non-black circles.

In addition, we examined a ratio algorithm R on the bases of three reflectance intensities at 557, 725, and 811 nm, as given in Eq. (2):

$$R = (R_{811} - R_{557})/(R_{725} - R_{557}) \tag{2}$$

Analysis of R images (Fig. 4C) indicated a better separation between uncontaminated and fecal contaminated skins than $Q_{725/557}$ images, and showed nearly the same effect of identifying fecal spots as $Q_{725/811}$ images. Although the R images provided more homogeneous background on uncontaminated apple surface than $Q_{725/811}$ images, they showed less contrast between uncontaminated and targeted fecal spots than $Q_{725/811}$ images.

To compare the results, three bands – 685, 722, and 869 nm-based asymmetric second difference algorithm was applied, because of its success in the detection of the diseased and contaminated spots on apple surfaces (Mehl et al., 2004). Asymmetric second difference (S'') was generalized using the following equation:

$$S'' = 0.2 * R_{685} - R_{722} + 0.8 * R_{869} \tag{3}$$

Fig. 4D shows the resultant images of asymmetric second difference, for comparison to the results shown in Fig. 4A–C. Notably, asymmetric second difference images provided clearer identification of fecal spots than $Q_{725/557}$ images, but in general revealed no better discrimination of fecal spots than $Q_{725/811}$ images, mainly because of large variations among apple surfaces.

Multivariate data analysis, namely principal component analysis (PCA), was also applied to identify the fecal spots from the apple images in full or narrow spectral regions. Careful examination of a number of principal component (PC) images revealed that there was no large difference in the detection of fecal spots between the full spectral region (450–950 nm) and the narrow region (688–895 nm). Fig. 4E shows the first PC image from the narrow region for the same apple set. As the first PC band explains more than 99% of eigenvalues, it contains the largest amounts of data variance. The first PC images can be seen to enhance the contrast between thick fecal spots (black) and uncontaminated skins (white), however, there were extensive difficulties in the detection of thin fecal spots.

3.4. Comparison of dual-band algorithms, second difference, and PCA models for the detection of fecal contaminants on Red Delicious apples

Hyperspectral images of Red Delicious apples were collected to examine the above observation. Fig. 5 shows the

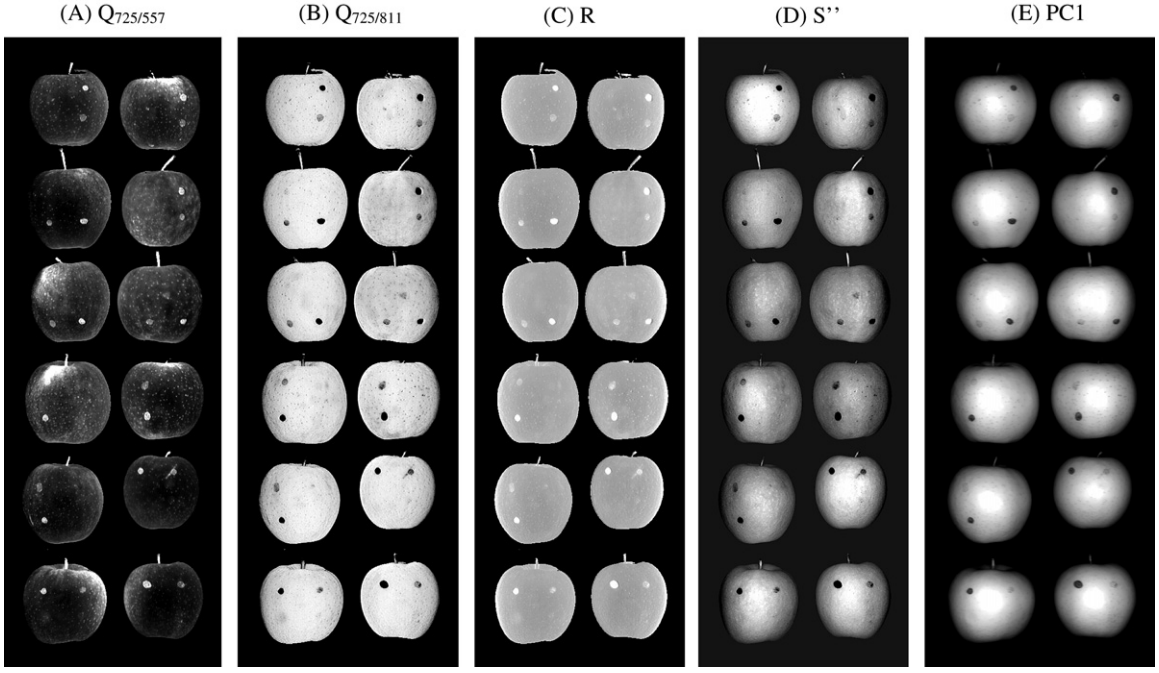

Fig. 4. Comparison of processed images of fecal contaminated Golden Delicious apples from dual-band ratio ($Q_{725/557}$) algorithm (A), dual-band ratio ($Q_{725/811}$) algorithm (B), three-band ratio algorithm (C), asymmetric second difference algorithm (D), and the first PC band (E).

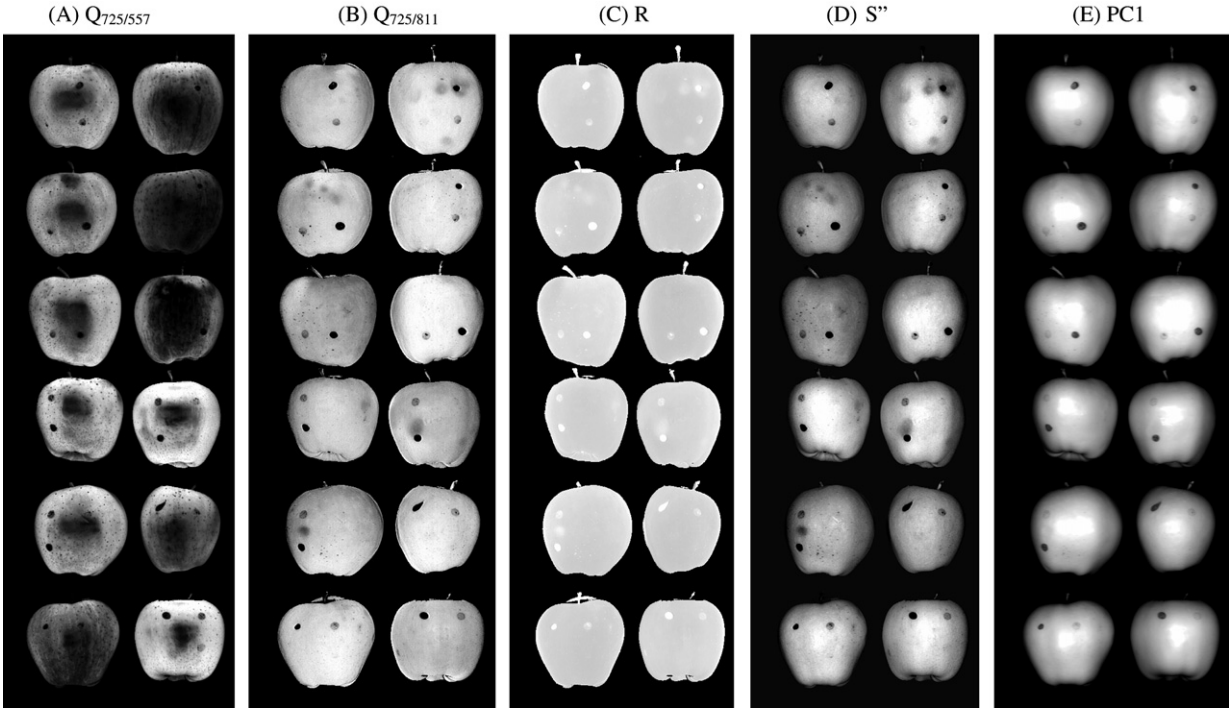

Fig. 5. Comparison of processed images of fecal contaminated Red Delicious apples from dual-band ratio ($Q_{725/557}$) algorithm (A), dual-band ratio ($Q_{725/811}$) algorithm (B), three-band ratio algorithm (C), asymmetric second difference algorithm (D), and the first PC band (E).

results of Red Delicious apples by using the same image processing strategies as given in Fig. 4. Similar to Golden Delicious apples, $Q_{725/811}$ algorithm images (Fig. 5B) provided the best discrimination power among the methods examined. Meanwhile, the $Q_{725/811}$ images indicated the easier and better determination of bruised apple skins than other processed images.

Comparison of the images in Figs. 4 and 5 suggested that fecal contaminated spots can be easily detected through a number of image analysis methods. Among them, the dual-band ratio ($Q_{725/811}$) algorithm images provided the best identification of thin and thick fecal spots. In other words, correct classification of fecal contaminants from simple dual-band ratio ($Q_{725/811}$) algorithm is well verified by both additional processing methods and the apples at different cultivars. Therefore, image analysis from the dual-band ratio algorithm is consistent, reliable, and effective. Major advantage of utilizing the 811 nm and 725 nm bands is to reduce the influence from the chlorophyll and carotenoids components.

4. Conclusions

The results of this study demonstrated the effectiveness of hyperspectral reflectance imaging technique in the characterization of uncontaminated and fecal contaminated apple skins. Reflectance intensities of ROI spectra of fecal contaminated apple skins decreased compared to those of uncontaminated skins. Great spectral differences between uncontaminated and fecal contaminated skins occurred in the 675–950 nm visible/NIR region, which provided the basis in developing simple algorithms for the detection of fecal contaminants on apple surfaces.

A number of image processing techniques were applied to analyze the images for the identification of fecal contaminated skins. The dual-band ratio ($Q_{725/811}$) algorithm yielded the best detection of fecal contaminated spots among the methods tested for two apple cultivars. The identification of the dual-band ratio ($Q_{725/811}$) algorithm is most important, because the two bands, 725 and 811 nm, are isolated from the absorptions of natural pigments (such as chlorophylls and carotenoids), and hence can reduce the effect of color variations (due to different apple cultivars) on the correct detection of fecal contaminated skins. Also, the algorithm was observed to be most useful for recognizing the bruised areas on apple skins. Consequently, the $Q_{725/811}$ algorithm, potentially as an universal and simple method, can be incorporated into a dual-band multispectral imaging system for the detection of fecal contaminants and bruises on different cultivars of apples.

Hyperspectral reflectance imaging technique only detected the fecal spots with higher amounts and/or concentrations, indicating a lack of sensitivity. Subsequent other researches have suggested that capability of determining the trace fecal spots was improved by using hyperspectral fluorescence imaging (Kim et al., 2002; Lefcourt, Kim, & Chen, 2005), which used a UV pulsed laser to excite samples and an intensified camera to record fluorescence response, due to relatively low quantum yield from fecal

matter. Undoubtedly, such a hyperspectral fluorescence system can greatly increase the order of detecting trace fecal portions, however, it might pick insignificant spots which are not from feces or are the feces but too tiny to be seen visually. In addition, both cost and stability of the excitation laser remains a question for real-time evaluation of apples during processing. Therefore, hyperspectral reflectance imaging is an option for practical implementation.

References

CDC. (1996). Outbreak of *Escherichia coli* O157:H7 infections associated with drinking unpasteurized commercial apple juice – British Columbia, California, Colorado, and Washington, October 1996. *Morbidity and Mortality Weekly Report*, *45*, 975.

CDC. (1997). Outbreak of *Escherichia coli* O157:H7 infections and cryptosporidiosis associated with drinking unpasteurized apple cider – Connecticut and New York, October 1996. *Morbidity and Mortality Weekly Report*, *46*, 4–8.

Cody, S. H., Glynn, M. K., Farrar, J. A., Cairns, K. L., Griffin, P. M., Kobayashi, J., et al. (1999). An outbreak of *Escherichia coli* O157:H7 infection from unpasteurized commercial apple Juice. *Annals of Internal Medicine, 130*, 202–209.

FDA. (1998). Guide to minimize microbial food safety hazards for fresh fruits and vegetables [Guidance for Industry]. <http://www.foodsafety.gov/~dms/prodguid.html>. Accessed 10.10.06.

FDA (2001). Hazard analysis and critical control point (HACCP): procedures for the safe and sanitary processing and importing of juices. *Federal Registry, 66*, 6137–6202.

Kim, M. S., Chen, Y. R., & Mehl, P. M. (2001). Hyperspectral reflectance and fluorescence imaging system for food quality and safety. *Transaction of the ASAE, 44*, 721–729.

Kim, M. S., Lefcourt, A. M., Chao, K., Chen, Y. R., Kim, I., & Chan, D. E. (2002). Multispectral detection of fecal contamination on apples based on hyperspectral imagery: Part I. Application of visible and near-infrared reflectance imaging. *Transaction of the ASAE, 45*, 2027–2037.

Kim, M. S., Lefcourt, A. M., Chen, Y. R., Kim, I., Chan, D. E., & Chao, K. (2002). Multispectral detection of fecal contamination on apples based on hyperspectral imagery: Part II. Application of hyperspectral fluorescence imaging. *Transaction of the ASAE, 45*, 2039–2047.

Lay, D. (2002). *Linear algebra and its applications*. New York: Addison-Wesley.

Lefcourt, A. M., Kim, M. S., & Chen, Y. R. (2005). Detection of fecal contamination on apples with nanosecond-scale time-resolved imaging of laser-induced fluorescence. *Applied Optics, 44*, 1160–1170.

Mehl, P. M., Chao, K., Kim, M. S., & Chen, Y. R. (2002). Detection of defects on selected apple cultivars using hyperspectral and multispectral image analysis. *Applied Engineering in Agriculture, 18*, 219–226.

Mehl, P. M., Chen, Y. R., Kim, M. S., & Chan, D. E. (2004). Development of hyperspectral imaging technique for the detection of apple surface defects and contaminations. *Journal of Food Engineering, 61*, 67–81.

Osborne, B. G., Fearn, T., & Hindle, P. H. (1993). *Practical near-infrared spectroscopy with application in food and beverage analysis* (2nd ed.). Harlow, UK: Longman Scientific & Technical.

Vargas, A. M., Kim, M. S., Tao, Y., Lefcourt, A. M., Chen, Y. R., Luo, Y., et al. (2005). Detection of fecal contamination on cantaloupes using hyperspectral fluorescence imagery. *Journal of Food Science, 70*, E471–E476.